

---

# BoGRAPE: BAYESIAN OPTIMIZATION OVER GRAPHS WITH SHORTEST-PATH ENCODED

---

Yilin Xie\*, Shiqiang Zhang\*, Jixiang Qing, Ruth Misener<sup>†</sup>, Calvin Tsay<sup>†</sup>  
 Department of Computing, Imperial College London  
 London, United Kingdom

## ABSTRACT

Graph-structured data play an important role across science and industry. This paper asks: how can we optimize over graphs, for instance to find the best graph structure and/or node features that minimize an expensive-to-evaluate black-box objective? Such problem settings arise, e.g., in molecular design, neural architecture search, and sensor placement. Bayesian optimization is a powerful tool for optimizing black-box functions, and existing technologies can be applied to optimize functions over nodes of a single fixed graph. We present Bayesian optimization acquisition functions for a class of shortest-path kernels and formulate them as mixed-integer optimization problems, enabling global exploration of the graph domain while maintaining solution feasibility when problem-specific constraints are present. We demonstrate our proposed approach, BoGrape, on several molecular design case studies.

## 1 Introduction

Graph-structured data are playing an emerging role across scientific and industrial fields, giving rise to a series of decision-making problems over graph domains, such as graph-based molecular design (Korovina et al., 2020; Mercado et al., 2021; Yang et al., 2024) and neural architecture search (Elsken et al., 2019; White et al., 2023). Broadly speaking, there are two classes of graph optimization problems (Wan et al., 2023): (i) *optimizing over nodes*, with a given (unknown) graph as the search space and a function over nodes as the objective, and (ii) *optimizing over graphs*, with the entire (constrained) graph domain as the search space and a function over graphs as the objective. The latter case, which this work studies, is usually more challenging since the graph structure itself is optimized, resulting in a complicated combinatorial optimization task.

For both aforementioned scenarios, the objective function can be a black-box, and, when expensive to evaluate, discourages gradient- and sampling-based methods. These characteristics motivate several works to extend Bayesian optimization (BO) (Frazier, 2018; Garnett, 2023) to graph domains (Cui and Yang, 2018; Oh et al., 2019; Wan et al., 2023; Liang et al., 2024) given its potential sample efficiency. BO relies on two main components: a surrogate model, e.g., Gaussian processes (GPs), trained on available data to approximate the underlying function, and an acquisition function used to suggest the next sample. To translate BO to graph domains, we require a surrogate model over graph inputs with suitable uncertainty quantification. Existing approaches mostly adopt GPs with various graph kernels (Ramachandram et al., 2017; Borovitskiy et al., 2021; Ru et al., 2021; Zhi et al., 2023). However, a general graph BO framework is missing since existing works either (i) limit the searchable graph set to a given fixed graph (Oh et al., 2019; Wan et al., 2023; Liang et al., 2024), directed labeled graphs (White et al., 2021; Ru et al., 2021; Wan et al., 2021), unlabeled graphs (Cui and Yang, 2018), etc. or (ii) rely on task-specific similarity metrics (Kandasamy et al., 2018).

When optimizing over graphs, no matter whether we optimize the graph function itself or its approximation, e.g., the BO acquisition function, the search space includes both continuous and discrete variables, thus limiting the choice of optimization techniques. For example, acquisition function optimization in graph BO is mostly solved using evolutionary algorithms (Kandasamy et al., 2018; Wan et al., 2021) or sampling (Ru et al., 2021; Wan et al., 2023), which are incapable of (i) efficiently exploring the search domain, (ii) proposing feasible solutions satisfying problem-specific

\*Equal contributions. Corresponding authors: yilin.xie22@imperial.ac.uk, s.zhang21@imperial.ac.uk

<sup>†</sup>Equal contributions.

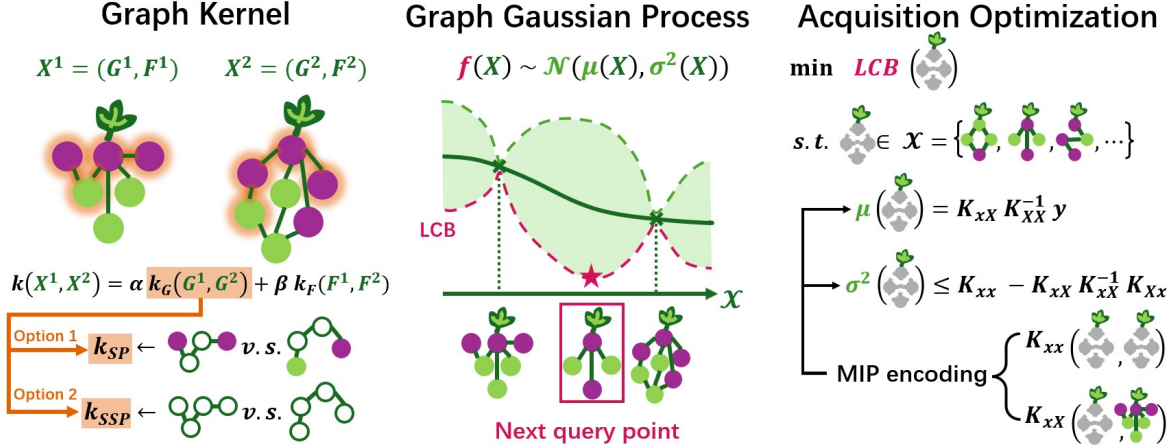


Figure 1: Key components of BoGrape. The **graph kernel** comprises  $k_G$  and  $k_F$  on the graph and feature levels, respectively. The **graph GP** is subsequently trained using the chosen kernel and samples. GP posterior information is used to build the acquisition function, e.g., LCB. Note that graph GP includes discrete graph domains; the continuous domain is only for illustration purposes. The **acquisition optimization** is formulated as a MIP using the encoding of shortest paths and graph kernels. Solving the MIP gives the next query point.

constraints, and (iii) guaranteeing optimality. To mitigate these issues, this paper explores mixed-integer programming (MIP) as an alternative option to represent an analytic expression of the graph function. The challenges this paper addresses are to manage both the black-box setting and the complicated form of surrogates via MIP for graph BO.

Recent advances on applying MIP to optimize trained machine learning (ML) models (Ceccon et al., 2022; Schweidtmann et al., 2022; Thebelt et al., 2022b) suggest pathways to address these challenges. By equivalently encoding surrogates, e.g., GPs (Schweidtmann et al., 2021), trees (Mišić, 2020; Mistry et al., 2021; Ammari et al., 2023), neural networks (NNs) (Fischetti and Jo, 2018; Anderson et al., 2020; Tsay et al., 2021; Wang et al., 2023), as constraints in larger decision-making problems, several MIP-based BO methods are proposed, allowing global optimization over mixed-feature domains (Thebelt et al., 2021, 2022a; Papalexopoulos et al., 2022; Xie et al., 2024). Moreover, some works develop MIP-based techniques to handle optimization problems constrained by graph neural networks (GNNs) with applications to molecular design (Zhang et al., 2023; McDonald et al., 2024; Zhang et al., 2024a) and robustness certification (Hojny et al., 2024). However, given the data requirements of GNNs, the computational cost of solving the large resulting MIPs, and the lack of uncertainty quantification, GNNs are impractical surrogates for graph BO.

This paper proposes BoGrape, a MIP-based graph BO method to optimize functions over connected graphs with attributes. GPs are chosen as the surrogates, using global acquisition function optimization methods introduced by Xie et al. (2024). We develop four variants of the classic shortest-path graph kernel (Borgwardt and Kriegel, 2005) for use in BoGrape. By precisely representing the shortest paths as decision variables, the acquisition function optimization is formulated as a MIP with a mixed-feature search space, graph kernel, and relevant problem-specific constraints. Figure 1 illustrates the BoGrape pipeline. To the best of our knowledge, BoGrape is the first BO algorithm addressing a general attributed graph domain and solving the acquisition function to global optimality.

**Paper structure:** Section 2 presents background knowledge. Section 3 introduces our method. Section 4 shows experimental results. Section 5 concludes and discusses future work. Appendix A contains theoretical results. Appendix B reports additional numerical details and results.

## 2 Preliminaries

### 2.1 Bayesian optimization

BO is a derivative-free optimization framework designed to iteratively approach the optimum of an expensive-to-evaluate, black-box function  $f : \mathcal{X} \rightarrow \mathbb{R}$  (Frazier, 2018). At each iteration, a surrogate model is trained on the current observed dataset  $\{(x_i, y_i)\}_{i=1}^{t-1}$  to learn a distribution over  $f$ . A common choice of surrogate is a GP (Schulz et al., 2018), a joint multivariate Gaussian distribution defined as:  $f \sim \mathcal{GP}(\mu(\cdot), k(\cdot, \cdot))$ , where  $\mu$  is the prior mean (often set to be zero), and  $k$  is the kernel function quantifying similarity between two inputs. Denote  $\mathbf{X} = [x_1, \dots, x_{t-1}]$  and  $\mathbf{y} = [y_1, \dots, y_{t-1}]$ , where  $y_i = f(x_i) + \epsilon$  is the noisy observation with  $\epsilon \sim \mathcal{N}(0, \sigma_\epsilon^2)$ . The posterior mean and

variance of the objective function value at  $x$  are given by:

$$\begin{aligned}\mu_t(x|\mathbf{X}, \mathbf{y}) &= K_{xX}(K_{XX} + \sigma_\epsilon^2 \mathbf{I})^{-1} \mathbf{y} \\ \sigma_t^2(x|\mathbf{X}, \mathbf{y}) &= K_{xx} - K_{xX}(K_{XX} + \sigma_\epsilon^2 \mathbf{I})^{-1} K_{Xx}\end{aligned}\quad (1)$$

where  $K_{XY} := K(\mathbf{X}, \mathbf{Y})$  for simplicity.

With the surrogate constructed and trained, an acquisition function is then formulated based on the posterior information, e.g., probability of improvement (PI) (Kushner, 1964), expected improvement (EI) (Jones et al., 1998), upper confidence bound (UCB) (Srinivas et al., 2010), predictive Entropy search (PES) (Hernández-Lobato et al., 2014), etc.. This paper uses the lower confidence bound (LCB) as the acquisition function, i.e., the minimization variant of UCB:

$$\alpha_{LCB}(x) = \mu_t(x) - \beta_t^{1/2} \sigma_t(x)$$

Optimizing the acquisition function returns the next query, whose function value is then evaluated to form the next data point. This process repeats until meeting some stopping criteria, e.g., the maximum iteration, time budget, etc..

## 2.2 Global optimization of acquisition functions

Most theoretical results for regret bounds in BO rely on the global optimization over acquisitions (Srinivas et al., 2012), i.e., they assume the global minimizer/maximizer of the acquisition function is found at each step, which may not be achieved using gradient- and sample-based optimizers. Xie et al. (2024) introduce PK-MIQP, a global acquisition optimization framework based on mixed-integer quadratic programming (MIQP). The core of PK-MIQP is the piecewise linearization of a stationary or dot-product kernel, e.g., RBF, Matérn, etc., based on which optimization of the acquisition function is then formulated as an MIQP:

$$\min_{x \in \mathcal{X}} \tilde{\mu} - \beta_t^{1/2} \tilde{\sigma} \quad (2a)$$

$$s.t. \tilde{\mu} = \tilde{K}_{xX} \tilde{K}_{XX}^{-1} \mathbf{y} \quad (2b)$$

$$\tilde{\sigma}^2 \leq \tilde{\sigma}_k^2 - \tilde{K}_{xX} \tilde{K}_{XX}^{-1} \tilde{K}_{Xx} \quad (2c)$$

$$r_i^2 = \frac{\|\mathbf{x} - \mathbf{x}_i\|_2^2}{l^2}, \forall 1 \leq i < t \quad (2d)$$

$$\tilde{K}_{xX_i} = \tilde{k}(r_i), \forall 1 \leq i < t \quad (2e)$$

where Eq. (2a) represents LCB,  $\tilde{\mu}$ ,  $\tilde{\sigma}^2$  in Eqs. (2a)–(2c) are the approximated mean and variance, respectively, calculated from the piecewise-linearized kernel  $\tilde{k}(\cdot)$  (the tildes denote the approximate representation of the kernel). Finally, Eq. (2e) contains an encoding of the piecewise-linear kernel. PK-MIQP is useful because of its (i) compatibility with various kernels (note the piecewise linearization is unnecessary if the kernel can be expressed linearly), and (ii) theoretical guarantee on regret bounds.

## 2.3 Graph kernels

Graph kernels extend the concept of kernels to graph domains and are used to evaluate the similarity between two graphs. Mathematically, a graph kernel  $k(\cdot, \cdot) : \mathcal{G} \times \mathcal{G} \rightarrow \mathbb{R}$  is given by  $k(G, G') = \langle \phi(G), \phi(G') \rangle_{\mathcal{H}}$ , where  $\phi : \mathcal{G} \rightarrow \mathcal{H}$  is a feature map from graph domain  $\mathcal{G}$  to a reproducing kernel Hilbert space  $\mathcal{H}$  with inner product  $\langle \cdot, \cdot \rangle_{\mathcal{H}}$  (Kriege et al., 2020). Past research develops graph kernels using a variety of graph patterns, e.g., neighborhoods, subgraphs, walks, paths. We refer the reader to Vishwanathan et al. (2010); Borgwardt et al. (2020); Kriege et al. (2020); Nikolentzos et al. (2021) for more details on graph kernels. Several works also use graph kernels to *optimize over nodes* (Oh et al., 2019; Borovitskiy et al., 2021; Wan et al., 2023; Liang et al., 2024), but the involved kernels measure the similarity of two nodes on *one given graph* and do not support *optimizing over graphs* (see Section 1 for this distinction).

# 3 Methodology

## 3.1 Shortest-path graph kernels

We focus on variants of the shortest-path (SP) kernel, owing to its ability to (i) handle both directed and undirected graphs, (ii) consider node labels, and (iii) capture the relationship between non-adjacent graph nodes, making it more general than kernels based on subgraph patterns, e.g., see Shervashidze et al. (2009); Costa and Grave (2010).

For graph  $G$ , denote  $l_u$  as the label of node  $u$ ,  $e_{u,v}$  as the shortest path from  $u$  to  $v$  (which may not be unique), and  $d_{u,v}$  as the shortest distance from node  $u$  to  $v$  (which is unique). Borgwardt and Kriegel (2005) define an SP kernel between graphs  $G^1 = (V^1, E^1)$  and  $G^2 = (V^2, E^2)$  as:

$$k_{SP}(G^1, G^2) = \sum_{u_1, v_1 \in V^1, u_2, v_2 \in V^2} k(e_{u_1, v_1}, e_{u_2, v_2})$$

$k(\cdot, \cdot)$  compares the labels and lengths of two shortest paths:

$$k(e_{u_1, v_1}, e_{u_2, v_2}) = k_v(l_{u_1}, l_{u_2}) \cdot k_e(d_{u_1, v_1}, d_{u_2, v_2}) \cdot k_v(l_{v_1}, l_{v_2})$$

where  $k_v$  is a kernel comparing node labels,  $k_e$  is a kernel comparing path lengths. Both  $k_v$  and  $k_e$  are usually chosen as Dirac kernels, giving the explicit representation of the SP kernel as:

$$k_{SP}(G^1, G^2) = \frac{1}{n_1^2 n_2^2} \sum_{u_1, v_1 \in V^1, u_2, v_2 \in V^2} \mathbf{1}(l_{u_1} = l_{u_2}) \cdot \mathbf{1}(d_{u_1, v_1} = d_{u_2, v_2}) \cdot \mathbf{1}(l_{v_1} = l_{v_2}) \quad (\text{SP})$$

where  $\frac{1}{n_1^2 n_2^2}$  is introduced as a normalizing coefficient with  $n_1, n_2$  as the number of nodes in graph  $G^1, G^2$ , respectively.

Note that each node may have more problem-specific features beyond a single label. From here on, we use  $X = (G, F)$  to denote an attributed graph with  $G$  as the underlying labeled graph and  $F$  as node features. Intuitively, we can compare the features of two nodes instead of labels in  $k_v$ . However, this could unnecessarily reduce the number of matching paths between two graphs, as requiring identical node features is restrictive and may introduce additional subgraph information into path comparison. Another option is to use a more complicated kernel  $k_v$  that measures similarity between features of two nodes, which may significantly increase the computational cost of optimization (similarity is computed for all node pairings). Therefore, we borrow from Cui and Yang (2018) the idea to separate the implicit and explicit information of graphs, i.e., the kernel value between two attributed graphs  $X^1, X^2$  becomes:

$$k(X^1, X^2) = \alpha \cdot k_G(G^1, G^2) + \beta \cdot k_F(F^1, F^2) \quad (3)$$

where  $k_G$  is any graph kernel,  $k_F$  is any kernel over features, and  $\alpha, \beta$  are trainable parameters controlling the trade-off between graph similarity and feature similarity. Appendix A.4 describes an example of  $k_F$ .

Since node label is usually included as a node feature and considered in  $k_F$  term, and comparing labels in Eq. (SP) increases the complexity of our optimization formulations, we propose a simplified shortest-path (SSP) kernel corresponding to an unlabeled SP kernel:

$$k_{SSP}(G^1, G^2) = \frac{1}{n_1^2 n_2^2} \sum_{u_1, v_1 \in V^1, u_2, v_2 \in V^2} \mathbf{1}(d_{u_1, v_1} = d_{u_2, v_2}) = \frac{1}{n_1^2 n_2^2} \sum_{0 \leq s < \min(n_1, n_2)} D_s(G^1) \cdot D_s(G^2) \quad (\text{SSP})$$

where  $D_s(G) := |\{(u, v) \mid u, v \in V, d_{u,v} = s\}|$  is the number of shortest paths with length  $s$  in graph  $G = (V, E)$ .

**Lemma 3.1.** *SP and SSP kernels are positive definite (PD).*

*Proof.* Borgwardt and Kriegel (2005) prove the SP kernel is PD. The SSP kernel is a special case of the SP kernel where all nodes have the same label, hence is also PD.  $\square$

Observe that both the SP and SSP kernels are linear kernels if we pre-process all shortest paths in each graph and count the number of each length of shortest path. Such linearity simplifies the optimization step (which still requires the non-trivial representation of shortest paths), but reduces the representation ability of the graph kernels and limits the maximal rank of the covariance matrix. Motivated by the practically strong performance of exponential kernels such as RBF kernel, Matérn kernel, graph diffusion kernel (Oh et al., 2019), etc., we propose the following two nonlinear graph kernels based on SP and SSP kernels:

$$k_{ESP}(G^1, G^2) = \exp(k_{SP}(G^1, G^2)) / \sigma_k^2 \quad (\text{ESP})$$

$$k_{ESSP}(G^1, G^2) = \exp(k_{SSP}(G^1, G^2)) / \sigma_k^2 \quad (\text{ESSP})$$

where variance  $\sigma_k^2$  is added to control the magnitude of kernel value. Note that we could also add variance to SP and SSP kernels, but it would be absorbed by  $\alpha, \beta$ .

**Lemma 3.2.** *ESP and ESSP kernels are PD.*

*Proof.* SP and SSP kernels can be rewritten into linear forms, so ESP and ESSP are exponential kernels, which are known to be PD (Fukumizu, 2010).  $\square$

The nonlinear kernels introduce additional difficulties for optimization as discussed in Section 3.4, but demonstrate better empirical performance compared to their linear counterparts, owing to increased representation ability.

### 3.2 Global acquisition optimization

We begin with the optimization formulation for the LCB acquisition function from Xie et al. (2024):

$$\min \mu - \beta_t^{1/2} \sigma \quad (5a)$$

$$\text{s.t. } \mu = K_{xX} K_{XX}^{-1} \mathbf{y} \quad (5b)$$

$$\sigma^2 \leq K_{xx} - K_{xX} K_{XX}^{-1} K_{Xx} \quad (5c)$$

$$K_{xX^i} = k(x, X^i), \forall 1 \leq i < t \quad (5d)$$

$$x = (G, F) \in \mathcal{X} = \mathcal{G} \times \mathcal{F} \quad (5e)$$

To maintain consistency with the general BO setting, we denote  $x = (G, F)$  as the next sample and  $X = \{(G^i, F^i), y^i\}_{i=1}^{t-1}$  as the prior samples at the  $t$ -th iteration. The difference is that now we need to optimize over both the graph domain  $G \in \mathcal{G}$  and the feature domain  $F \in \mathcal{F}$ . W.l.o.g., assume that each node has  $M$  features, i.e.,  $F^i \in \mathbb{R}^{n(G^i) \times M}$ , and the first  $L$  features denote the one-hot encoding of its label, i.e.,  $\sum_{l \in [L]} F_l^i = 1, \forall 1 \leq i < t$ , where we use  $[n]$  to denote set  $\{0, 1, \dots, n-1\}$ .

The advantages of formulation Eq. (5) are: (i) it is compatible with discrete variables, a key challenge of graph optimization, (ii) Eq. (5e) allows problem-specific constraints over the graph domain, (iii) Eq. (5d) is generic to the choice of graph kernel, and (iv) nonlinear kernels can be piecewise-linearly approximated and incorporated into Eq. (5) with theoretical guarantees on regret bounds.

A binary adjacency matrix is sufficient to represent the graph domain, but encoding the shortest path between any two nodes is not straightforward and is one of the major contributions of this work. We first introduce the formulation of shortest paths in Section 3.3 and then explicitly derive Eq. (5d) in Section 3.4 for the graph kernels in Section 3.1.

### 3.3 Encoding of the shortest paths

For the sake of exposition, we start with all connected graphs  $G$  with fixed size, i.e., node number  $n$  is given. Appendix A.3 discusses formulations for graphs of unknown size.

Table 1 summarizes the optimization variables. We now describe the optimization formulation for graph kernels, which involve constant graph information and their variable counterparts. For each variable  $Var$ , we use  $Var(G)$  to denote its value on a given graph  $G$ . For example,  $d_{u,v}(G)$  is the shortest distance from node  $u$  to node  $v$  in graph  $G$ .

If graph  $G$  is given, all variables in Table 1 can be computed using classic shortest-path algorithms, such as the Floyd–Warshall algorithm (Floyd, 1962). In graph optimization tasks, however, we need to encode the relationships between these variables as constraints. Motivated by the Floyd–Warshall algorithm, we first present the constraints in Eq. (6) and then prove that there exists a bijective between the feasible domain given by these constraints and all connected graphs with size  $n$ .

$$A_{v,v} = 1, \quad \forall v \quad (6a)$$

$$d_{v,v} = 0, \quad \forall v \quad (6b)$$

$$d_{u,v} \begin{cases} = 1, & A_{u,v} = 1 \\ > 1, & A_{u,v} = 0 \end{cases}, \quad \forall u \neq v \quad (6c)$$

$$d_{u,v} \begin{cases} = d_{u,w} + d_{w,v}, & \delta_{u,v}^w = 1 \\ < d_{u,w} + d_{w,v}, & \delta_{u,v}^w = 0 \end{cases}, \quad \forall u \neq v \quad (6d)$$

$$\delta_{v,v}^w = \begin{cases} 1, & w = v \\ 0, & w \neq v \end{cases}, \quad \forall v \quad (6e)$$

$$\delta_{u,v}^u = \delta_{u,v}^v = 1, \quad \forall u \neq v \quad (6f)$$

$$\sum_{w \in [n]} \delta_{u,v}^w \begin{cases} = 2, & A_{u,v} = 1 \\ > 2, & A_{u,v} = 0 \end{cases}, \quad \forall u \neq v \quad (6g)$$

Eq. (6) are necessary conditions that  $A_{u,v}, d_{u,v}, \delta_{u,v}^w$  should satisfy, using the big-M method to represent the disjunctive constraints in a linear formulation. Appendix A.2 explains the constraints in detail. Here we directly give the final

Table 1: List of variables introduced to represent the shortest path, where  $n$  is the number of nodes.

variables	type	description
$A_{u,v} \in \{0, 1\}, u, v \in [n]$	binary	the existence of edge from node $u$ to $v$
$d_{u,v} \in [n], u, v \in [n]$	integer	the length of shortest path from node $u$ to $v$
$\delta_{u,v}^w \in \{0, 1\}, u, v, w \in [n]$	binary	if node $w$ appears at the shortest path from node $u$ to $v$

encoding of the shortest paths in the following linear MIP:

$$\left\{ \begin{array}{ll}
 A_{v,v} = 1, & \forall v \\
 d_{v,v} = 0, & \forall v \\
 d_{u,v} \leq 1 + n \cdot (1 - A_{u,v}), & \forall u \neq v \\
 d_{u,v} \geq 2 - A_{u,v}, & \forall u \neq v \\
 d_{u,v} \leq d_{u,w} + d_{w,v} - (1 - \delta_{u,v}^w), & \forall u, v, w \\
 d_{u,v} \geq d_{u,w} + d_{w,v} - 2n \cdot (1 - \delta_{u,v}^w), & \forall u, v, w \\
 \delta_{v,v}^v = 1, & \forall v \\
 \delta_{v,v}^w = 0, & \forall w \neq v \\
 \delta_{u,v}^u = \delta_{u,v}^v = 1, & \forall u \neq v \\
 \sum_{w \in [n]} \delta_{u,v}^w \leq 2 + (n - 2) \cdot (1 - A_{u,v}), & \forall u \neq v \\
 \sum_{w \in [n]} \delta_{u,v}^w \geq 2 + (1 - A_{u,v}), & \forall u \neq v
 \end{array} \right. \quad (\text{MIP-SP})$$

**Lemma 3.3.**  $(A_{u,v}(G), d_{u,v}(G), \delta_{u,v}^w(G))$  is a feasible solution of Eq. (MIP-SP) with size  $n = n(G)$  given any connected graph  $G$ .

*Proof.* Trivial to verify by definition.  $\square$

**Theorem 3.4.** Given any  $n \in \mathbb{Z}^+$ , for any feasible solution  $(A_{u,v}, d_{u,v}, \delta_{u,v}^w)$  of Eq. (MIP-SP) with size  $n$ , there exists a unique graph  $G$  such that:

$$(A_{u,v}(G), d_{u,v}(G), \delta_{u,v}^w(G)) = (A_{u,v}, d_{u,v}, \delta_{u,v}^w)$$

i.e., there is a bijective between the feasible domain of Eq. (MIP-SP) with size  $n$  and the set consisting of all connected graphs with  $n$  nodes.

The formulation becomes more complicated when the graph size is unknown (but bounded). Denote  $n_0$  and  $n$  as the minimal and maximal number of nodes, respectively, and use  $A_{v,v}$  to represent the existence of node  $v$ . We need to assign proper values to  $d_{u,v}$  and  $\delta_{u,v}^w$  when either of  $u$  or  $v$  does not exist. Moreover, we extend the domain of  $d_{u,v}$  from  $[n]$  to  $[n + 1]$  and use  $n$  to denote infinity. Eq. (MIP-SP-plus) in Appendix A.3 presents the encoding and Theorem 3.5 extends Theorem 3.4 to unknown size.

**Theorem 3.5.** There is a bijective between the feasible domain of Eq. (MIP-SP-plus) with size  $[n_0, n]$  and all connected graphs with number of nodes in  $[n_0, n]$ .

See Appendix A for proofs of Theorems 3.4 and 3.5. These theorems guarantee the equivalence of our encoding for directed graphs. Appendix A.5 shows how to further simplify our encoding for undirected graphs.

### 3.4 Encoding of graph kernels

We now rewrite Eq. (5d) using Eq. (3) as:

$$K_{xX_i} = k(x, X_i) = \alpha \cdot k_G(G, G^i) + \beta \cdot k_F(F, F^i)$$

Given that  $k_F$  is independent of the choice of graph kernel  $k_G$ , and that kernels on continuous features are studied in Xie et al. (2024), here we focus on formulating  $k_G$ . See Appendix A.4 for kernel encoding with binary features, which are relatively less considered in continuous scenarios.

With the shortest distances  $d_{u,v}$  as decision variables, formulating  $k_G(G, G_i)$  is straightforward for SP and SSP kernels:

$$k_{SSP}(G, G^i) = \frac{1}{n^2 n_i^2} \sum_{u_1, v_1 \in [n]} \sum_{u_2, v_2 \in [n(G^i)]} d_{u_1, v_1}^{d_{u_2, v_2}(G^i)} = \frac{1}{n^2 n_i^2} \sum_{u, v, s \in [n]} D_s(G^i) \cdot d_{u, v}^s$$

where  $n_i := n(G^i)$  is the number of nodes of  $G^i$  and  $d_{u, v}^s = \mathbf{1}(d_{u, v} = s)$  are indicator variables of a big-M formulation:

$$\sum_{s \in [n+1]} d_{u, v}^s = 1, \quad \sum_{s \in [n+1]} s \cdot d_{u, v}^s = d_{u, v}, \quad \forall u, v \in [n]$$

*Remark 3.6.* We introduce  $d_{u, v}^s$  for  $s \in [n+1]$  instead of  $s \in [n]$  to include the cases with unknown graph size, where  $d_{u, v} = n$  means the shortest path from node  $u$  to  $v$  does not exist. But  $d_{u, v}^n$  is not used in evaluating the kernel.

Similarly, introducing indicator variables  $p_{u, v}^{s, l_1, l_2}$  as:

$$p_{u, v}^{s, l_1, l_2} = \mathbf{1}(F_{u, l_1} = 1, d_{u, v} = s, F_{v, l_2} = 1), \quad \forall u, v, s \in [n], l_1, l_2 \in [L]$$

and counting the numbers of each type of paths in  $G^i$ :

$$P_{s, l_1, l_2}(G^i) = |\{(u, v) \mid u, v \in [n_i], l_u(G^i) = l_1, d_{u, v}(G^i) = s, l_v(G^i) = l_2\}|$$

the SP kernel is formulated as:

$$k_{SP}(G, G^i) = \frac{1}{n^2 n_i^2} \sum_{u, v, s \in [n], l_1, l_2 \in [L]} P_{s, l_1, l_2}(G^i) \cdot p_{u, v}^{s, l_1, l_2}$$

There are several ways to handle the exponential kernels: (i) directly use (local) nonlinear solvers, losing optimality guarantees, (ii) piecewise linearize the exponential function following Xie et al. (2024), or (iii) utilize nonlinear MIP functionalities in established solvers such as Gurobi (Gurobi Optimization, LLC, 2024) or SCIP (Vigerske and Gleixner, 2018). In our experiments, we choose to use Gurobi, which by default employs a dynamic piecewise linear approximation of the exponential function.

It is noteworthy that  $K_{xx}$  in Eq. (5c) is not constant with a non-stationary kernel, making it the most complicated term in the whole formulation. By definition,  $k_{SSP}(G, G)$  has the following quadratic form:

$$k_{SSP}(G, G) = \frac{1}{n^4} \sum_{s \in [n]} D_s^2$$

where  $D_s = \sum_{u, v \in [n]} d_{u, v}^s, \forall s \in [n]$ . Reusing the indicator trick and introducing  $D_s^c = \mathbf{1}(D_s = c), \forall s \in [n], c \in [n^2 + 1]$ , the quadratic form is equivalently linearized as:

$$K_{SSP}(G, G) = \frac{1}{n^4} \sum_{s \in [n], c \in [n^2+1]} c^2 \cdot D_s^c$$

where indicator variables should satisfy:

$$\sum_{c \in [n^2+1]} D_s^c = 1, \quad \sum_{c \in [n^2+1]} c \cdot D_s^c = D_s, \quad \forall s \in [n]$$

Repeating the procedure for SP kernel, we have:

$$K_{SP}(G, G) = \frac{1}{n^4} \sum_{s \in [n], l_1, l_2 \in [L], c \in [n^2+1]} c^2 \cdot P_{s, l_1, l_2}^c$$

where indicator variables  $P_{s, l_1, l_2}^c = \mathbf{1}(P_{s, l_1, l_2} = c)$  satisfy:

$$\sum_{c \in [n^2+1]} P_{s, l_1, l_2}^c = 1, \quad \sum_{c \in [n^2+1]} c \cdot P_{s, l_1, l_2}^c = P_{s, l_1, l_2}, \quad \forall s \in [n], l_1, l_2 \in [L]$$

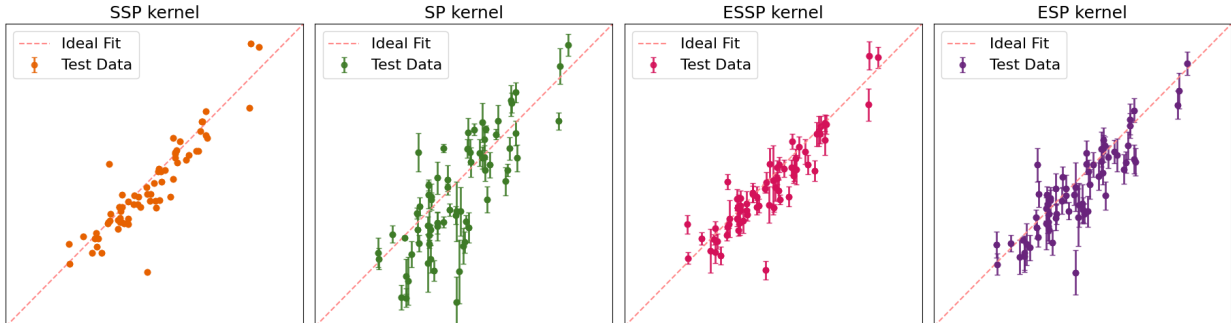


Figure 2: Compare predictive performance of GP with different kernels. 100 samples are randomly chosen from the QM7 dataset with various graph sizes, 30 of which are used for training. The predictive mean with one standard deviation (predicted  $y$ ) of the remaining 70 graphs are plotted against their real values (true  $y$ ).

Table 2: Model performance of GPs equipped with different graph kernels. For each graph size  $N$ , we use Limeade to random generate 20 and 100 molecules for training and testing, respectively, root mean square error (RMSE) of predictive error is reported over 30 replications.

$N$	QM7				QM9			
	SSP	SP	ESSP	ESP	SSP	SP	ESSP	ESP
10	0.30(0.08)	0.28(0.06)	0.29(0.08)	<b>0.26(0.07)</b>	1.20(0.47)	<b>0.67(0.13)</b>	0.85(0.24)	0.68(0.12)
15	0.30(0.09)	<b>0.21(0.05)</b>	0.23(0.07)	<b>0.21(0.06)</b>	1.27(0.68)	0.45(0.16)	0.78(0.30)	<b>0.44(0.16)</b>
20	0.32(0.14)	<b>0.22(0.08)</b>	0.26(0.08)	0.23(0.08)	1.41(0.69)	0.56(0.16)	0.82(0.35)	<b>0.55(0.15)</b>
25	<b>0.19(0.08)</b>	<b>0.19(0.07)</b>	0.25(0.08)	0.22(0.08)	0.57(0.41)	<b>0.34(0.20)</b>	0.45(0.31)	0.35(0.21)
30	0.28(0.19)	<b>0.26(0.15)</b>	0.34(0.19)	0.31(0.17)	0.24(0.26)	<b>0.20(0.19)</b>	0.25(0.26)	0.23(0.24)

## 4 Experiments

Since most graph BO works focus on specific types of graphs, there are few synthetic benchmarks available. We choose the optimal molecular design task studied in Zhang et al. (2023); McDonald et al. (2024) since (i) molecules can be represented as attributed, connected graphs, (ii) molecular properties, either measured or predicted, are suitable functions over graphs, and (iii) the MIP-based framework for molecular design is well-established. Specifically, we use datasets QM7 (Blum and Reymond, 2009; Rupp et al., 2012) and QM9 (Ruddigkeit et al., 2012; Ramakrishnan et al., 2014) as real-world case studies, each of which consists of molecules with quantum mechanic properties. Each molecule is represented as a graph with  $F = 15$  node features, including  $L = 4$  labels. Since the maximal size of molecules is 7 and 9 for QM7 and QM9, respectively, we follow Zhang et al. (2023) and train a GNN as a predictor for each dataset. We choose  $\beta_t^{1/2} = 1$  defined in Eq. (5a).

All experiments are performed on a 4.2 GHz Intel Core i7-7700K CPU with 16 GB memory. We use GPflow (Matthews et al., 2017) to implement GP models, PyG (Fey and Lenssen, 2019) to implement GNNs, and Gurobi v11.0.0 (Gurobi Optimization, LLC, 2024) to solve MIPs. Random sampling is a common baseline, but is excluded here since it rarely produces even feasible solutions. Instead, we use the recently released open-source tool Limeade (Zhang et al., 2024b) to randomly generate feasible molecules, which is further enhanced by incorporating the composition constraints and symmetry-breaking constraints proposed by Zhang et al. (2023). Appendix B.2 compares random sampling and Limeade. From here on, we use (random) sampling to mean generating feasible molecules using Limeade.

### 4.1 Model performance

Before conducting the optimization task, we test the performance of GPs with the four graph kernels. There are two trainable parameters, i.e.,  $\alpha, \beta$ , for the SP and SSP kernels, and one extra variance  $\sigma_k^2$  for the two exponential kernels.

We consider two settings based on the molecular size  $N$ : (a) if the dataset includes molecules of size  $N$ , we randomly choose molecules from the dataset and use their real properties, and (b) for larger  $N$ , we use Limeade to generate molecules and use the trained GNN to predict their properties. To show the performance of different kernels on representing similarity between graphs, we apply setting (a) and perform a property prediction task using GPs equipped

**Algorithm 1** BoGrape at  $t$ -th iteration.

- 1: **Input:**
- 2: dataset  $X = \{(G^i, F^i), y^i\}_{i=1}^{t-1}$ , hyperparameter  $\beta_t$ ,
- 3: graph kernel  $\in \{\text{SSP}, \text{SP}, \text{ESSP}, \text{ESP}\}$ .
- 4: **Model training:**
- 5: kernel parameters  $\alpha, \beta, \sigma_k^2 \leftarrow$  graph GP fit to  $X$ .
- 6: **Acquisition formulation:**
- 7: define objective in Eq. (5a)  $\leftarrow$  definition of LCB.
- 8: represent  $K_{xX^i}$  in Eqs. (5b) – (5d)  $\leftarrow$  Section 3.4.
- 9: encode  $K_{xx}$  in Eq. (5c)  $\leftarrow$  Section 3.4.
- 10: search space  $\mathcal{X}$  in Eq. (5e)  $\leftarrow$  problem-specific.
- 11: **Optimization:**
- 12: initialize MIP Eq. (5)  $\leftarrow$  warm start (optional).
- 13: optimal solution  $(G^t, F^t) \leftarrow$  solve Eq. (5).
- 14: **Output:** proposed sample  $(G^t, F^t)$ .

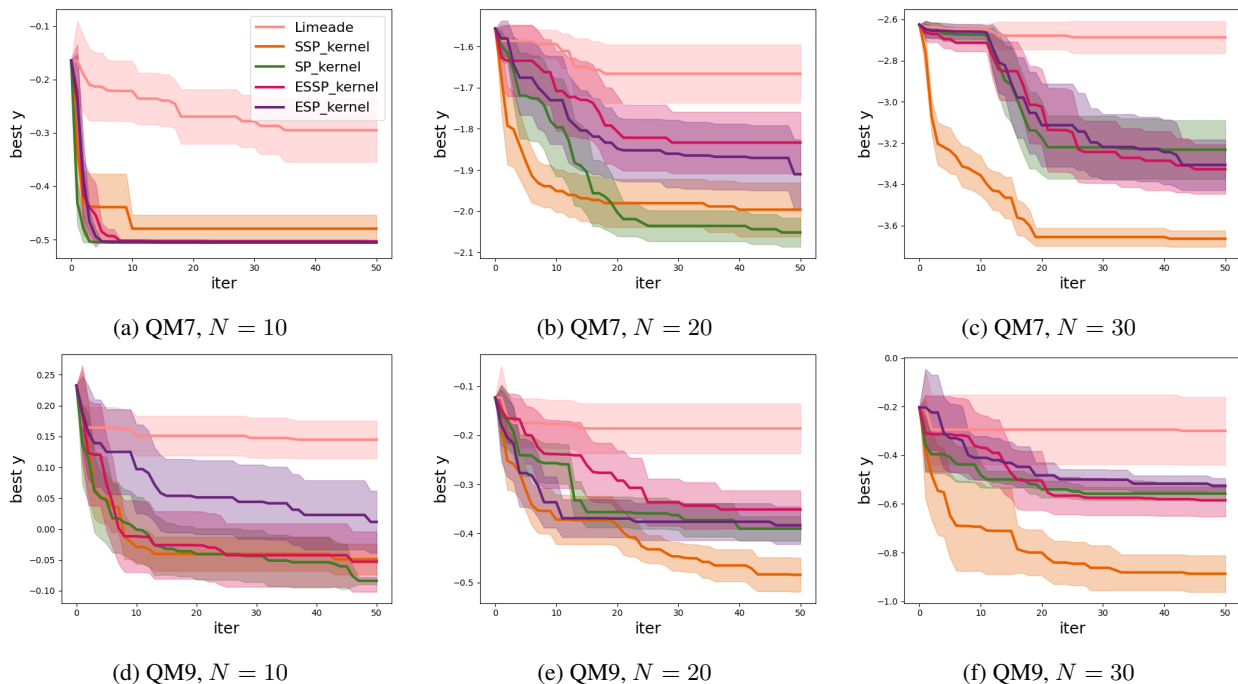


Figure 3: Bayesian optimization results on QM7 and QM9 with  $N \in \{10, 20, 30\}$ . Best objective value is plotted at each iteration. Mean with 0.5 standard deviation over 10 replications is reported.

with the various kernels, shown in Figure 2. For larger graph sizes, we apply setting (b) and report the root mean square errors (RMSE) of GP regression in Table 2.

From Figure 2 we conclude the four graph kernels have comparable prediction performance in terms of accuracy, while two exponential kernels, i.e., ESSP and ESP, may more accurately quantify uncertainty. When graph size  $N$  is larger, Table 2 shows that the more complicated kernels, i.e., SP and ESP, are generally better at predicting graph properties since they impose stronger criteria on comparing shortest-paths between two graphs. Table 4 in Appendix B.1 gives the mean negative log likelihoods (MNLs).

**4.2 Optimal molecular design**

Now we have presented all the pieces needed to implement an end-to-end BO procedure. We employ the trained GNNs used in Section 4.1 as oracle predictors, i.e., the functions that we seek to optimize. At each iteration, we train a GP with a graph kernel and extract trained model parameters  $\alpha, \beta, \sigma_k^2$  to calculate  $K_{XX}$  and represent  $K_{xx}, K_{xX_i}$  appearing in

Eqs. (5b)–(5d). Eq. (5e) defines the search domain, which is already set up in Zhang et al. (2024a). Solving the final MIP suggests the next molecule to query.

Although molecular design is a promising and important application area for BO (Paulson and Tsay, 2024), our proposed BoGrape procedure is general for any setting with functions defined over connected graphs. Algorithm 1 outlines BoGrape, where we include an optional warm start before solving Eq. (5). During the warm start at each iteration, 20 randomly sampled feasible molecules, together with previously sampled molecules, are used to initialize the global solution algorithm with some feasible solutions, i.e., good primal solutions. In our experiments, 10 random molecules sampled by Limeade are used as the initial dataset, and 50 BO iterations are performed. We set PoolSearchMode=2 in Gurobi to generate feasible solutions using Limeade. For each BO run, we show the mean with 0.5 standard deviation of the best objective value over 10 replications. When solving Eq. (5), we observed decent solutions to be found early (since more time is spent on proving optimality) and set 600s as the MIP time limit.

The computational results in Figure 3 show that BoGrape outperforms Limeade regardless of which graph kernel is used. The SSP kernel displays the best performance in most cases, especially when the graph size  $N$  is large. This observation suggests that this simpler encoding reduces model complexity and produces better solutions within the given computational time. The SP kernel, which includes stricter comparison between graphs and has outstanding predictive performance as shown in Table 2, outperforms the SSP kernel in some cases, e.g. Figures 3a, 3b, 3d. Exponential kernels have good representation ability, at the trade-off that their formulations result in more complicated MIPs and require more computational resources for good performance. We hypothesize that BO with the exponential kernels may be more capable of providing high-quality solutions giving longer computational time.

## 5 Conclusion

This work proposes BoGrape to optimize black-box functions over graphs. Four shortest-path graph kernels are presented and tested on both prediction and Bayesian optimization tasks. The underlying mixed-integer formulation provides a flexible and general platform including mixed-feature search spaces, graph kernels, acquisition functions, and problem-specific constraints. Our results show promising performance and suggest trade-offs between query-efficiency and computational time when choosing a suitable kernel. Future work may further simplify the formulations and adapt BoGrape to more applications such as network architecture search.

## Acknowledgments

The authors gratefully acknowledge support from a Department of Computing Scholarship (YX), BASF SE, Ludwigshafen am Rhein (SZ), Engineering and Physical Sciences Research Council [grant numbers EP/W003317/1 and EP/X025292/1] (RM, CT, JQ), a BASF/RAEng Research Chair in Data-Driven Optimisation (RM), a BASF/RAEng Senior Research Fellowship (CT).

## References

- B. L. Ammari, E. S. Johnson, G. Stinchfield, T. Kim, M. Bynum, W. E. Hart, J. Pulsipher, and C. D. Laird. Linear model decision trees as surrogates in optimization of engineering applications. *Computers & Chemical Engineering*, 178, 2023.
- R. Anderson, J. Huchette, W. Ma, C. Tjandraatmadja, and J. P. Vielma. Strong mixed-integer programming formulations for trained neural networks. *Mathematical Programming*, 183(1):3–39, 2020.
- L. C. Blum and J.-L. Reymond. 970 million druglike small molecules for virtual screening in the chemical universe database GDB-13. *Journal of the American Chemical Society*, 131(25):8732–8733, 2009.
- K. Borgwardt, E. Ghisu, F. Llinares-López, L. O’Bray, B. Rieck, et al. Graph kernels: State-of-the-art and future challenges. *Foundations and Trends® in Machine Learning*, 13(5-6):531–712, 2020.
- K. M. Borgwardt and H.-P. Kriegel. Shortest-path kernels on graphs. In *International Conference on Data Mining*, 2005.
- V. Borovitskiy, I. Azangulov, A. Terenin, P. Mostowsky, M. P. Deisenroth, and N. Durrande. Matern Gaussian processes on graphs. In *International Conference on Artificial Intelligence and Statistics*, 2021.
- F. Ceccon, J. Jalving, J. Haddad, A. Thebelt, C. Tsay, C. D. Laird, and R. Misener. OMLT: Optimization & machine learning toolkit. *Journal of Machine Learning Research*, 23(1):15829–15836, 2022.
- F. Costa and K. D. Grave. Fast neighborhood subgraph pairwise distance kernel. In *ICML*, 2010.

- J. Cui and B. Yang. Graph Bayesian optimization: Algorithms, evaluations and applications. *arXiv preprint arXiv:1805.01157*, 2018.
- T. Elsken, J. H. Metzen, and F. Hutter. Neural architecture search: a survey. *Journal of Machine Learning Research*, 2019.
- M. Fey and J. E. Lenssen. Fast graph representation learning with PyTorch Geometric. In *ICLR 2019 Workshop on Representation Learning on Graphs and Manifolds*, 2019.
- M. Fischetti and J. Jo. Deep neural networks and mixed integer linear optimization. *Constraints*, 23(3):296–309, 2018.
- R. W. Floyd. Algorithm 97: Shortest path. *Communications of the ACM*, 5(6):345–345, 1962.
- P. I. Frazier. A tutorial on Bayesian optimization. *arXiv preprint arXiv:1807.02811*, 2018.
- K. Fukumizu. Kernel method: Data analysis with positive definite kernels. *Graduate University of Advanced Studies*, 2010.
- R. Garnett. *Bayesian Optimization*. Cambridge University Press, 2023.
- Gurobi Optimization, LLC. Gurobi optimizer reference manual, 2024. URL <https://www.gurobi.com>.
- J. M. Hernández-Lobato, M. W. Hoffman, and Z. Ghahramani. Predictive entropy search for efficient global optimization of black-box functions. *NeurIPS*, 2014.
- C. Hojny, S. Zhang, J. S. Campos, and R. Misener. Verifying message-passing neural networks via topology-based bounds tightening. In *ICML*, 2024.
- D. R. Jones, M. Schonlau, and W. J. Welch. Efficient global optimization of expensive black-box functions. *Journal of Global Optimization*, 13:455–492, 1998.
- K. Kandasamy, W. Neiswanger, J. Schneider, B. Póczos, and E. P. Xing. Neural architecture search with Bayesian optimisation and optimal transport. *NeurIPS*, 31, 2018.
- K. Korovina, S. Xu, K. Kandasamy, W. Neiswanger, B. Póczos, J. Schneider, and E. Xing. Chembo: Bayesian optimization of small organic molecules with synthesizable recommendations. In *AISTATS*, 2020.
- N. M. Kriege, F. D. Johansson, and C. Morris. A survey on graph kernels. *Applied Network Science*, 5:1–42, 2020.
- H. J. Kushner. A new method of locating the maximum point of an arbitrary multipeak curve in the presence of noise. *Journal of Basic Engineering*, 86(1):97–106, 1964.
- H. Liang, X. Wan, and X. Dong. Bayesian optimization of functions over node subsets in graphs. *arXiv preprint arXiv:2405.15119*, 2024.
- A. G. d. G. Matthews, M. van der Wilk, T. Nickson, K. Fujii, A. Boukouvalas, P. León-Villagrà, Z. Ghahramani, and J. Hensman. GPflow: A Gaussian process library using TensorFlow. *Journal of Machine Learning Research*, 18(40): 1–6, 2017.
- T. McDonald, C. Tsay, A. M. Schweidtmann, and N. Yorke-Smith. Mixed-integer optimisation of graph neural networks for computer-aided molecular design. *Computers & Chemical Engineering*, 185:108660, 2024.
- R. Mercado, T. Rastemo, E. Lindelöf, G. Klambauer, O. Engkvist, H. Chen, and E. J. Bjerrum. Graph networks for molecular design. *Machine Learning: Science and Technology*, 2021.
- V. V. Mišić. Optimization of tree ensembles. *Operations Research*, 68(5):1605–1624, 2020.
- M. Mistry, D. Letsios, G. Krennrich, R. M. Lee, and R. Misener. Mixed-integer convex nonlinear optimization with gradient-boosted trees embedded. *INFORMS Journal on Computing*, 33(3):1103–1119, 2021.
- G. Nikolentzos, G. Siglidis, and M. Vazirgiannis. Graph kernels: A survey. *Journal of Artificial Intelligence Research*, 72:943–1027, 2021.
- C. Oh, J. Tomczak, E. Gavves, and M. Welling. Combinatorial Bayesian optimization using the graph cartesian product. *NeurIPS*, 2019.
- T. P. Papalexopoulos, C. Tjandraatmadja, R. Anderson, J. P. Vielma, and D. Belanger. Constrained discrete black-box optimization using mixed-integer programming. In *International Conference on Machine Learning*, pages 17295–17322. PMLR, 2022.
- J. A. Paulson and C. Tsay. Bayesian optimization as a flexible and efficient design framework for sustainable process systems. *Current Opinion in Green and Sustainable Chemistry*, page 100983, 2024.
- D. Ramachandram, M. Lisicki, T. J. Shields, M. R. Amer, and G. W. Taylor. Structure optimization for deep multimodal fusion networks using graph-induced kernels. *arXiv preprint arXiv:1707.00750*, 2017.

- R. Ramakrishnan, P. O. Dral, M. Rupp, and O. A. Von Lilienfeld. Quantum chemistry structures and properties of 134 kilo molecules. *Scientific Data*, 1(1):1–7, 2014.
- B. Ru, X. Wan, X. Dong, and M. Osborne. Interpretable neural architecture search via Bayesian optimisation with Weisfeiler-Lehman kernels. In *ICLR*, 2021.
- L. Ruddigkeit, R. Van Deursen, L. C. Blum, and J.-L. Reymond. Enumeration of 166 billion organic small molecules in the chemical universe database gdb-17. *Journal of Chemical Information and Modeling*, 52(11):2864–2875, 2012.
- M. Rupp, A. Tkatchenko, K.-R. Müller, and O. A. Von Lilienfeld. Fast and accurate modeling of molecular atomization energies with machine learning. *Physical Review Letters*, 108(5):058301, 2012.
- E. Schulz, M. Speekenbrink, and A. Krause. A tutorial on Gaussian process regression: Modelling, exploring, and exploiting functions. *Journal of mathematical psychology*, 85, 2018.
- A. M. Schweidtmann, D. Bongartz, D. Grothe, T. Kerkenhoff, X. Lin, J. Najman, and A. Mitsos. Deterministic global optimization with Gaussian processes embedded. *Mathematical Programming Computation*, 13(3):553–581, 2021.
- A. M. Schweidtmann, D. Bongartz, and A. Mitsos. Optimization with trained machine learning models embedded. In *Encyclopedia of Optimization*, pages 1–8. Springer, 2022.
- N. Shervashidze, S. Vishwanathan, T. Petri, K. Mehlhorn, and K. Borgwardt. Efficient graphlet kernels for large graph comparison. In *AISTATS*, 2009.
- N. Srinivas, A. Krause, S. Kakade, and M. Seeger. Gaussian process optimization in the bandit setting: No regret and experimental design. In *ICML*, 2010.
- N. Srinivas, A. Krause, S. M. Kakade, and M. W. Seeger. Information-theoretic regret bounds for Gaussian process optimization in the bandit setting. *IEEE Transactions on Information Theory*, 58:3250–3265, 2012.
- A. Thebelt, J. Kronqvist, M. Mistry, R. M. Lee, N. Sudermann-Merx, and R. Misener. Entmoot: A framework for optimization over ensemble tree models. *Computers & Chemical Engineering*, 151:107343, 2021.
- A. Thebelt, C. Tsay, R. M. Lee, N. Sudermann-Merx, D. Walz, T. Tranter, and R. Misener. Multi-objective constrained optimization for energy applications via tree ensembles. *Applied Energy*, 306:118061, 2022a.
- A. Thebelt, J. Wiebe, J. Kronqvist, C. Tsay, and R. Misener. Maximizing information from chemical engineering data sets: Applications to machine learning. *Chemical Engineering Science*, 252:117469, 2022b.
- C. Tsay, J. Kronqvist, A. Thebelt, and R. Misener. Partition-based formulations for mixed-integer optimization of trained ReLU neural networks. In *NeurIPS*, 2021.
- S. Vigerske and A. Gleixner. SCIP: Global optimization of mixed-integer nonlinear programs in a branch-and-cut framework. *Optimization Methods and Software*, 33(3):563–593, 2018.
- S. V. N. Vishwanathan, N. N. Schraudolph, R. Kondor, and K. M. Borgwardt. Graph kernels. *The Journal of Machine Learning Research*, 11:1201–1242, 2010.
- X. Wan, H. Kenlay, B. Ru, A. Blaas, M. Osborne, and X. Dong. Adversarial attacks on graph classifiers via Bayesian optimisation. In *NeurIPS*, 2021.
- X. Wan, P. Osselin, H. Kenlay, B. Ru, M. A. Osborne, and X. Dong. Bayesian optimisation of functions on graphs. *NeurIPS*, 2023.
- K. Wang, L. Lozano, C. Cardonha, and D. Bergman. Optimizing over an ensemble of trained neural networks. *INFORMS Journal on Computing*, 2023.
- C. White, W. Neiswanger, and Y. Savani. Bananas: Bayesian optimization with neural architectures for neural architecture search. In *AAAI*, 2021.
- C. White, M. Safari, R. Sukthanker, B. Ru, T. Elsken, A. Zela, D. Dey, and F. Hutter. Neural architecture search: insights from 1000 papers. *arXiv preprint arXiv:2301.08727*, 2023.
- Y. Xie, S. Zhang, J. Paulson, and C. Tsay. Global optimization of Gaussian process acquisition functions using a piecewise-linear kernel approximation. *arXiv preprint arXiv:2410.16893*, 2024.
- N. Yang, H. Wu, K. Zeng, Y. Li, S. Bao, and J. Yan. Molecule generation for drug design: a graph learning perspective. *Fundamental Research*, 2024.
- S. Zhang, J. S. Campos, C. Feldmann, D. Walz, F. Sandfort, M. Mathea, C. Tsay, and R. Misener. Optimizing over trained GNNs via symmetry breaking. In *NeurIPS*, 2023.
- S. Zhang, J. S. Campos, C. Feldmann, F. Sandfort, M. Mathea, and R. Misener. Augmenting optimization-based molecular design with graph neural networks. *Computers & Chemical Engineering*, 186:108684, 2024a.

*BoGrape*, Xie and Zhang, et al.

S. Zhang, C. W. Feldmann, F. Sandfort, M. Mathea, J. S. Campos, and R. Misener. Limeade: Let integer molecular encoding aid. *arXiv preprint arXiv:2411.16623*, 2024b.

Y.-C. Zhi, Y. C. Ng, and X. Dong. Gaussian processes on graphs via spectral kernel learning. *IEEE Transactions on Signal and Information Processing over Networks*, 2023.

## A Encoding of graph kernels

### A.1 Notations

We provide details for all variables introduced in this paper in Table 3. Recall that the search domain considered here consists of all connected graphs with node number ranging from  $n_0$  to  $n$ , each node has  $M$  binary features with the first  $L$  node features as the one-hot encoding of node label.

Table 3: All variables introduced in the optimization formulation for graph kernels.

Variables	Domain	Number	Description
$A_{u,v}, u, v \in [n]$	$\{0, 1\}$	$n^2$	the existence of edge from $u$ to $v$
$d_{u,v}, u, v \in [n]$	$[n + 1]$	$n^2$	the length of shortest path from $u$ to $v$
$\delta_{u,v}^w, u, v, w \in [n]$	$\{0, 1\}$	$n^3$	if $w$ appears at the shortest path from $u$ to $v$
$d_{u,v}^s, u, v \in [n], s \in [n + 1]$	$\{0, 1\}$	$n^2(n + 1)$	indicator: $\mathbf{1}(d_{u,v} = s)$
$D_s, s \in [n]$	$[n^2 + 1]$	$n$	# shortest paths with length $s$
$D_s^c, s \in [n], c \in [n^2 + 1]$	$\{0, 1\}$	$n(n^2 + 1)$	indicator: $\mathbf{1}(D_s = c)$
$p_{u,v}^{s,l_1,l_2}, u, v, s \in [n], l_1, l_2 \in [L]$	$\{0, 1\}$	$n^3L^2$	indicator: $\mathbf{1}(F_{u,l_1} = 1, d_{u,v} = s, F_{v,l_2} = 1)$
$P_{s,l_1,l_2}, s \in [n], l_1, l_2 \in [L]$	$[n^2 + 1]$	$nL^2$	# shortest paths with length $s$ and labels $l_1, l_2$
$P_{s,l_1,l_2}^c, s \in [n], l_1, l_2 \in [L], c \in [n^2 + 1]$	$\{0, 1\}$	$n(n^2 + 1)L^2$	indicator: $\mathbf{1}(P_{s,l_1,l_2} = c)$
$N^m, m \in [M]$	$[N + 1]$	$M$	sum of $m$ -th feature over all nodes
$N_m^c, m \in [M], c \in [M + 1]$	$\{0, 1\}$	$M(M + 1)$	indicator: $\mathbf{1}(N_m = c)$

### A.2 Shortest path encoding for graphs with fixed size

Eq. (6) restricts  $A_{u,v}, d_{u,v}, \delta_{u,v}^w$  in the following rules:

- Eq. (6a) initializes the diagonal elements.
- Eq. (6b) initializes the shortest distance from  $v$  to itself.
- Eq. (6c) forces the shortest distance from node  $u$  and  $v$  be 1 if edge  $u \rightarrow v$  exists, and larger than 1 otherwise. Rewrite Eq. (6c) as:

$$\begin{aligned} d_{u,v} &\leq 1 + n \cdot (1 - A_{u,v}), & \forall u \neq v \in [n] \\ d_{u,v} &\geq 2 - A_{u,v}, & \forall u \neq v \in [n] \end{aligned}$$

where  $n$  is a big-M coefficient using  $d_{u,v} \leq n - 1$ .

- Eq. (6d) is the triangle inequality for distance matrix  $d$ . Rewrite Eq. (6d) as:

$$\begin{aligned} d_{u,v} &\leq d_{u,w} + d_{w,v} - (1 - \delta_{u,v}^w), & \forall u, v, w \\ d_{u,v} &\geq d_{u,w} + d_{w,v} - 2n \cdot (1 - \delta_{u,v}^w), & \forall u, v, w \end{aligned}$$

where  $2n$  is a big-M coefficient since  $d_{u,w} + d_{w,v} < 2n$ .

- Eq. (6e) initializes  $\delta_{v,v}^w$  by definition.
- Eq. (6f) initializes  $\delta_{u,v}^u$  and  $\delta_{u,v}^v$  by definition.
- Eq. (6g) ensures that there is at least one node at the shortest path from node  $u$  to  $v$  if there is no edge from node  $u$  to  $v$ . Otherwise, no node except for  $u$  and  $v$  could appear at the shortest path from  $u$  to  $v$ . Rewrite Eq. (6g) as:

$$\begin{aligned} \sum_{w \in [n]} \delta_{u,v}^w &\leq 2 + (n - 2) \cdot (1 - A_{u,v}), & \forall u \neq v \\ \sum_{w \in [n]} \delta_{u,v}^w &\geq 2 + (1 - A_{u,v}), & \forall u \neq v \end{aligned}$$

where  $n - 2$  is a big-M coefficient since  $\sum_{w \in [n]} \delta_{u,v}^w \leq n$ .

Replacing disjunctive constraints accordingly in Eq. (6) gives the final formulation Eq. (MIP-SP).

*Proof of Theorem 3.4.* If such  $G$  exists, it is unique since  $A_{u,v}$  gives the existence of every edge. Thus it suffices to show that  $(d_{u,v}(G), \delta_{u,v}^w(G)) = (d_{u,v}, \delta_{u,v}^w)$  for  $G$  defined with  $A_{u,v}$ .

We are going to prove it by induction on the shortest distance  $sd$  from node  $u$  to  $v$  in graph  $G$ . Specifically, we want to show that for any  $0 \leq sd < n$ , and for any pair of  $(u, v)$  such that  $\min(d_{u,v}(G), d_{u,v}) = sd$ , we have  $d_{u,v}(G) = d_{u,v}$  and  $\delta_{u,v}^w(G) = \delta_{u,v}^w, \forall w \in [n]$ .

For  $sd = 0$ ,  $\min(d_{u,v}(G), d_{u,v}) = 0$  if and only if  $u = v$ . For any  $v \in [n]$ , it is obvious to have:

$$\begin{aligned} d_{v,v}(G) &= 0 = d_{v,v} \\ \delta_{v,v}^v(G) &= 1 = \delta_{v,v}^v \\ \delta_{v,v}^w(G) &= 0 = \delta_{v,v}^w, \forall w \neq v \end{aligned}$$

For  $sd = 1$ , consider every pair  $(u, v)$  such that  $d_{u,v}(G) = 1$ , we have  $A_{u,v} = A_{u,v}(G) = 1$ , then it is easy to obtain:

$$\begin{aligned} d_{u,v}(G) &= 1 = d_{u,v} \\ \delta_{u,v}^w(G) &= 1 = \delta_{u,v}^w, \forall w \in \{u, v\} \\ \delta_{u,v}^w(G) &= 0 = \delta_{u,v}^w, \forall w \notin \{u, v\} \end{aligned}$$

where  $\delta_{u,v}^w = 0, \forall w \notin \{u, v\}$  since:

$$\sum_{w \notin \{u, v\}} \delta_{u,v}^w = \sum_{w \in [n]} \delta_{u,v}^w - \delta_{u,v}^u - \delta_{u,v}^v = 0$$

On the contrary,  $d_{u,v} = 1$  gives  $A_{u,v} = 1$ , thus  $A_{u,v}(G) = 1$  and  $\delta_{u,v}^w(G) = \delta_{u,v}^w, \forall w$  by definition.

Now assume that for any pair of  $(u, v)$  such that  $\min(d_{u,v}(G), d_{u,v}) \leq sd$ , we have  $d_{u,v}(G) = d_{u,v}$  and  $\delta_{u,v}^w(G) = \delta_{u,v}^w, \forall w$ . Since  $\delta_{u,v}^w(G) = \delta_{u,v}^w, \forall w \in \{u, v\}$  always holds by definition, we only consider  $w \notin \{u, v\}$ .

**Part 1:** We first consider every pair of  $(u, v)$  such that  $d_{u,v}(G) = sd + 1$ . Since  $sd + 1 \geq 2$ , we know that  $A_{u,v} = A_{u,v}(G) = 0$  and there exists  $w \notin \{u, v\}$  on the shortest path from node  $u$  to  $v$  in graph  $G$ .

*Case 1.1:* For every  $w \notin \{u, v\}$  such that  $\delta_{u,v}^w(G) = 1$ , since  $d_{u,w}(G) \leq sd$  and  $d_{w,v}(G) \leq sd$ , we have:

$$d_{u,v} \leq d_{u,w} + d_{w,v} = d_{u,w}(G) + d_{w,v}(G) = d_{u,v}(G) = sd + 1$$

The equality has to hold, otherwise,  $d_{u,v} \leq sd$  gives  $d_{u,v}(G) = d_{u,v} \leq sd$  by assumption. Therefore,  $\delta_{u,v}^w = 1 = \delta_{u,v}^w(G)$ .

*Case 1.2:* For every  $w \notin \{u, v\}$  such that  $\delta_{u,v}^w(G) = 0$ , if  $\delta_{u,v}^w = 1$ , then  $d_{u,w} + d_{w,v} = d_{u,v} = sd + 1$ , which means that  $d_{u,w} \leq sd$  and  $d_{w,v} \leq sd$ . By assumption, we have  $d_{u,w}(G) = d_{u,w}, d_{w,v}(G) = d_{w,v}$  and then:

$$d_{u,w}(G) + d_{w,v}(G) = d_{u,w} + d_{w,v} = d_{u,v} = d_{u,v}(G)$$

which contradicts to  $\delta_{u,v}^w(G) = 0$ . Thus  $\delta_{u,v}^w = 0$ .

**Part 2:** Then we consider every pair of  $(u, v)$  such that  $d_{u,v} = sd + 1$ . Similarly, we have  $A_{u,v} = A_{u,v}(G) = 0$ .

*Case 2.1:* For every  $w \notin \{u, v\}$  such that  $\delta_{u,v}^w = 1$ , since  $d_{u,w} \leq sd$  and  $d_{w,v} \leq sd$ , we have  $d_{u,w}(G) = d_{u,w}$  and  $d_{w,v}(G) = d_{w,v}$ , then:

$$d_{u,v}(G) \leq d_{u,w}(G) + d_{w,v}(G) = d_{u,w} + d_{w,v} = d_{u,v} = sd + 1$$

This equality also has to hold, otherwise,  $d_{u,v}(G) \leq sd$ , by assumption  $d_{u,v} = d_{u,v}(G) \leq sd$ , which is a contradiction.

*Case 2.2:* For every  $w \notin \{u, v\}$  such that  $\delta_{u,v}^w = 0$ , if  $\delta_{u,v}^w(G) = 1$ , then  $d_{u,w}(G) = d_{w,v}(G) = d_{u,v}(G) = sd + 1$ , which means that  $d_{u,w}(G) \leq sd$  and  $d_{w,v}(G) \leq sd$ . Therefore,

$$d_{u,w} + d_{w,v} = d_{u,w}(G) + d_{w,v}(G) = d_{u,v}(G) = d_{u,v}$$

which contradicts to  $\delta_{u,v}^w = 0$ . □

### A.3 Shortest path encoding for graph with unknown size

We extend constraints listed in Eq. (6) to handle changeable graph size. Full constraints are shown as follows:

$$A_{v,v} \geq A_{v+1,v+1}, \quad \forall v \in [n-1] \quad (7a)$$

$$\sum_{v \in [n]} A_{v,v} \geq n_0, \quad (7b)$$

$$2A_{u,v} \leq A_{u,u} + A_{v,v}, \quad \forall u \neq v \in [n] \quad (7c)$$

$$d_{v,v} = 0, \quad \forall v \in [n] \quad (7d)$$

$$d_{u,v} \begin{cases} = 1, & A_{u,v} = 1 \\ > 1, & A_{u,v} = 0 \end{cases}, \quad \forall u \neq v \in [n] \quad (7e)$$

$$d_{u,v} \begin{cases} < n, & A_{u,u} = A_{v,v} = 1 \\ = n, & \min\{A_{u,u}, A_{v,v}\} = 1 \end{cases}, \quad \forall u \neq v \in [n] \quad (7f)$$

$$d_{u,v} \begin{cases} = d_{u,w} + d_{w,v}, & \delta_{u,v}^w = 1 \\ < d_{u,w} + d_{w,v}, & \delta_{u,v}^w = 0 \end{cases}, \quad \forall u \neq v \in [n] \quad (7g)$$

$$\delta_{v,v}^w = \begin{cases} 1, & w = v \\ 0, & w \neq v \end{cases}, \quad \forall v \in [n] \quad (7h)$$

$$\delta_{u,v}^u = \delta_{u,v}^v = 1, \quad \forall u \neq v \in [n] \quad (7i)$$

$$\sum_{w \in [n]} \delta_{u,v}^w \begin{cases} = 2, & A_{u,v} = 1 \\ > 2, & A_{u,v} = 0, A_{u,u} = A_{v,v} = 1 \\ = 2, & \min\{A_{u,u}, A_{v,v}\} = 0 \end{cases}, \quad \forall u \neq v \in [n] \quad (7j)$$

- Eq. (7a) forces nodes with smaller indexes exist.
- Eq. (7b) gives the lower bound of the number of existed nodes.
- Eq. (7c) means that there is no edge from node  $u$  to  $v$  if any of them does not exist.
- Eq. (7d) initializes the shortest distance from one node to itself, even this node does not exist.
- Eq. (7e) forces the shortest distance from node  $u$  and  $v$  be 1 if there is one edge from  $u$  to  $v$ , and larger than 1 otherwise.

Rewrite Eq. (7e) as:

$$\begin{aligned} d_{u,v} &\leq 1 + n \cdot (1 - A_{u,v}), & \forall u \neq v \in [n] \\ d_{u,v} &\geq 2 - A_{u,v}, & \forall u \neq v \in [n] \end{aligned}$$

where  $n$  is a big-M coefficient using the fact that  $d_{u,v} \leq n$ .

- Eq. (7f) sets the shortest distance from node  $u$  to  $v$  as  $n$ , i.e.,  $\infty$ , if any of them does not exist. Otherwise, the shortest distance is less than  $n$ .

Rewrite Eq. (7f) as:

$$\begin{aligned} d_{u,v} &\geq n \cdot (1 - A_{u,u}), & \forall u \neq v \in [n] \\ d_{u,v} &\geq n \cdot (1 - A_{v,v}), & \forall u \neq v \in [n] \end{aligned}$$

- Eq. (7g) is the triangle inequality for the distance matrix  $d$ .

Rewrite Eq. (7g) as:

$$\begin{aligned} d_{u,v} &\leq d_{u,w} + d_{w,v} - (1 - \delta_{u,v}^w), & \forall u, v, w \in [n] \\ d_{u,v} &\geq d_{u,w} + d_{w,v} - 2n \cdot (1 - \delta_{u,v}^w), & \forall u, v, w \in [n] \end{aligned}$$

where  $2n$  is a big-M coefficient since  $d_{u,w} + d_{w,v} \leq 2n$ .

- Eq. (7h) initializes  $\delta_{v,v}^w$  by definition, even node  $v$  does not exist.
- Eq. (7i) initializes  $\delta_{u,v}^u$  and  $\delta_{u,v}^v$  by definition, even node  $u$  or  $v$  does not exist.
- Eq. (7j) makes sure that there is at least one node at the shortest path from node  $u$  to  $v$  if there is no edge from node  $u$  and  $v$  and these two nodes both exist. Otherwise, only  $\delta_{u,v}^u$  and  $\delta_{u,v}^v$  equal to 1.

Rewrite Eq. (7j) as:

$$\begin{aligned}
\sum_{w \in [n]} \delta_{u,v}^w &\leq 2 + (n-2) \cdot (1 - A_{u,v}), & \forall u \neq v \in [n] \\
\sum_{w \in [n]} \delta_{u,v}^w &\leq 2 + (n-2) \cdot A_{u,u}, & \forall u \neq v \in [n] \\
\sum_{w \in [n]} \delta_{u,v}^w &\leq 2 + (n-2) \cdot A_{v,v}, & \forall u \neq v \in [n] \\
\sum_{w \in [n]} \delta_{u,v}^w &\geq A_{u,u} + A_{v,v} + (1 - A_{u,v}), & \forall u \neq v \in [n]
\end{aligned}$$

where  $n-2$  is a big-M coefficient since  $\sum_{w \in [n]} \delta_{u,v}^w \leq n$ .

To conclude, the formulation for shortest paths of all connected graphs with at least  $n_0$  nodes and at most  $n$  nodes is:

$$\left\{ \begin{array}{ll}
A_{v,v} \geq A_{v+1,v+1}, & \forall v \in [n-1] \\
\sum_{v \in [n]} A_{v,v} \geq n_0, & \\
2A_{u,v} \leq A_{u,u} + A_{v,v}, & \forall u \neq v \in [n] \\
d_{v,v} = 0, & \forall v \in [n] \\
d_{u,v} \leq 1 + n \cdot (1 - A_{u,v}), & \forall u \neq v \in [n] \\
d_{u,v} \geq 2 - A_{u,v}, & \forall u \neq v \in [n] \\
d_{u,v} \geq n \cdot (1 - A_{u,u}), & \forall u \neq v \in [n] \\
d_{u,v} \geq n \cdot (1 - A_{v,v}), & \forall u \neq v \in [n] \\
d_{u,v} \leq d_{u,w} + d_{w,v} - (1 - \delta_{u,v}^w), & \forall u, v, w \in [n] \\
d_{u,v} \geq d_{u,w} + d_{w,v} - 2n \cdot (1 - \delta_{u,v}^w), & \forall u, v, w \in [n] \\
\delta_{v,v}^w = \begin{cases} 1, & w = v \\ 0, & w \neq v \end{cases}, & \forall v \in [n] \\
\delta_{u,v}^u = \delta_{u,v}^v = 1, & \forall u \neq v \in [n] \\
\sum_{w \in [n]} \delta_{u,v}^w \leq 2 + (n-2) \cdot (1 - A_{u,v}), & \forall u \neq v \in [n] \\
\sum_{w \in [n]} \delta_{u,v}^w \leq 2 + (n-2) \cdot A_{u,u}, & \forall u \neq v \in [n] \\
\sum_{w \in [n]} \delta_{u,v}^w \leq 2 + (n-2) \cdot A_{v,v}, & \forall u \neq v \in [n] \\
\sum_{w \in [n]} \delta_{u,v}^w \geq A_{u,u} + A_{v,v} + (1 - A_{u,v}), & \forall u \neq v \in [n]
\end{array} \right. \quad (\text{MIP-SP-plus})$$

*Proof of Theorem 3.5.* Fix the node number as  $n_1$  with  $n_0 \leq n_1 \leq n$ , Eqs. (7a) – (7b) force:

$$A_{v,v} = \begin{cases} 1, & v \in [n_1] \\ 0, & v \in [n] \setminus [n_1] \end{cases}$$

substituting which to other constraints give us:

$$\begin{aligned}
A_{u,v} = A_{v,u} = 0, & \quad \forall u \neq v, u \in [n_1], v \in [n] \setminus [n_1] \\
d_{v,v} = 0, & \quad \forall v \in [n] \setminus [n_1] \\
d_{u,v} = d_{v,u} = n, & \quad \forall u \neq v, u \in [n_1], v \in [n] \setminus [n_1] \\
\delta_{u,v}^w = \delta_{v,u}^w = \begin{cases} 1, & w \in \{u, v\} \\ 0, & w \notin \{u, v\} \end{cases}, & \quad \forall u \in [n_1], v \in [n] \setminus [n_1]
\end{aligned}$$

One can easily check that all constraints associated with non-existed nodes are satisfied. Removing those constraints turns Eq. (MIP-SP-plus) into Eq. (MIP-SP) with size  $n_1$ .  $\square$

#### A.4 Encoding for kernel over binary features

Assume that each graph  $G$  has a binary feature matrix  $F \in \{0, 1\}^{n(G) \times M}$ , we need to formulate  $k_F(F, F^i)$  and  $k_F(F, F)$  properly.  $k_F$  could be defined in multiple ways, here we propose a permutational-invariant kernel considering the pair-wise similarity among node features. Given two feature matrices  $F^1, F^2$  corresponding to graphs  $G^1, G^2$  respectively, define  $k_F$  as:

$$k_F(F^1, F^2) := \frac{1}{n_1 n_2 M} \sum_{v_1 \in V^1, v_2 \in V^2} F_{v_1}^1 \cdot F_{v_2}^2 = \frac{1}{n_1 n_2 M} \sum_{m \in [M]} N_m(F^1) \cdot N_m(F^2)$$

where  $N_m(F) = |\{v \mid v \in G, F_{v,m} = 1\}|$ ,  $\forall m \in [M]$ ,  $\frac{1}{n_1 n_2 M}$  is the normalized coefficient.

Similar to Section 3.4, we have:

$$k_F(F, F^i) = \frac{1}{n n_i M} \sum_{m \in [M]} N_m(F^i) \cdot N_m$$

where  $N_m = \sum_{v \in [n]} F_{v,m}$ ,  $\forall m \in [M]$ , and

$$k_F(F, F) = \frac{1}{n^2 M} \sum_{m \in [M]} N_m^2 = \frac{1}{n^2 M} \sum_{m \in [M], c \in [M+1]} c^2 \cdot N_m^c$$

where indicators  $N_m^c = \mathbf{1}(N_m = c)$ ,  $\forall m \in [M], c \in [M+1]$  satisfy:

$$\sum_{c \in [M+1]} N_m^c = 1, \quad \sum_{c \in [M+1]} c \cdot N_m^c = N_m, \quad \forall m \in [M]$$

#### A.5 Simplify path encoding over undirected graphs

For undirected graphs, we first add the following constraints to guarantee symmetry:

$$\begin{cases} A_{u,v} = A_{v,u}, & \forall u < v \in [n] \\ d_{u,v} = d_{v,u}, & \forall u < v \in [n] \\ \delta_{u,v}^w = \delta_{v,u}^w, & \forall u < v \in [n], w \in [n] \end{cases}$$

Since the inverse of any shortest path from node  $u$  to  $v$  is also a shortest path from node  $v$  to  $u$ , for SSP and ESSP kernels,  $D_s$ ,  $\forall s \in [n]$  are even and we can fix odd indicators as zero:

$$D_s^c = \begin{cases} 1, & c \text{ is even} \\ 0, & c \text{ is odd} \end{cases}, \quad \forall s \in [n], c \in [n^2 + 1]$$

Similarly, for SP and ESP kernels, we have:

$$P_{s,l_1,l_2} = P_{s,l_2,l_1}, \quad \forall s \in [n], f_1, f_2 \in [L]$$

Table 4: Model performance of GPs equipped with different graph kernels. For each graph size  $N$ , we use Limeade to random generate 20 and 100 molecules for training and testing, respectively, mean negative log likelihood (MNLL) is reported over 30 replications.

DATASET	$N$	SSP	SP	ESSP	ESP
QM7	10	6098.53(3475.83)	4.56(5.47)	0.59(0.57)	<b>0.19(0.46)</b>
	15	472.75(414.04)	1.06(1.71)	1.12(1.31)	<b>0.12(0.52)</b>
	20	440.53(418.42)	2.92(5.07)	2.47(3.37)	<b>0.27(0.60)</b>
	25	309.44(344.72)	10.06(16.12)	2.77(3.58)	<b>0.06(0.74)</b>
	30	581.49(621.67)	197.80(254.26)	1.64(2.33)	<b>0.87(1.71)</b>
QM9	10	116087.28(62728.04)	2.00(0.93)	2.58(1.05)	<b>1.23(0.42)</b>
	15	15756.72(18864.45)	1.26(0.98)	1.66(0.98)	<b>0.63(0.77)</b>
	20	7618.60(6860.77)	1.36(0.82)	2.45(2.13)	<b>0.97(0.42)</b>
	25	1065.96(1907.33)	1.15(2.92)	0.62(2.78)	<b>-0.59(1.91)</b>
	30	61.50(148.76)	-0.06(4.93)	-1.28(3.50)	<b>-1.88(2.82)</b>

## B Additional numerical results

### B.1 Kernel performance

All GPs are trained by maximizing the log marginal likelihood. During GP training, we set bounds for kernel parameters, i.e.,  $\alpha, \beta, \sigma_k^2$ , to  $[0.01, 100]$  with 1 as their initial values, and set noise variance  $\sigma_\epsilon^2$  as  $10^{-6}$ . Besides the RMSE performance in Table 2, we further report the mean negative log likelihood (MNLL) of GPs with different kernels and graph sizes in Table 4. ESSP and ESP have smaller MNLL values, showing that exponential graph kernels provide better uncertainty measurement.

### B.2 Random sampling v.s. Limeade

Randomly sample feasible graphs is not trivial because the graph structure and features should be reasonable and compatible with each other, e.g., satisfying structural feasibility, dataset-specific constraints, etc. in molecular generation task. Here we consider random sampling over QM7 and QM9, to guarantee the feasibility of samples and compare it with Limeade. Figure 4 plots the regret curve over 50 iterations for both sample methods. In all cases, Limeade outperforms random sampling, showing the limitations of random sampling. Therefore, we choose Limeade as our sampling baseline.

### B.3 Additional optimal molecular design results

Experimental results for  $N \in \{15, 25\}$  are reported in Figure 5, supporting our analysis in Section 4.2.

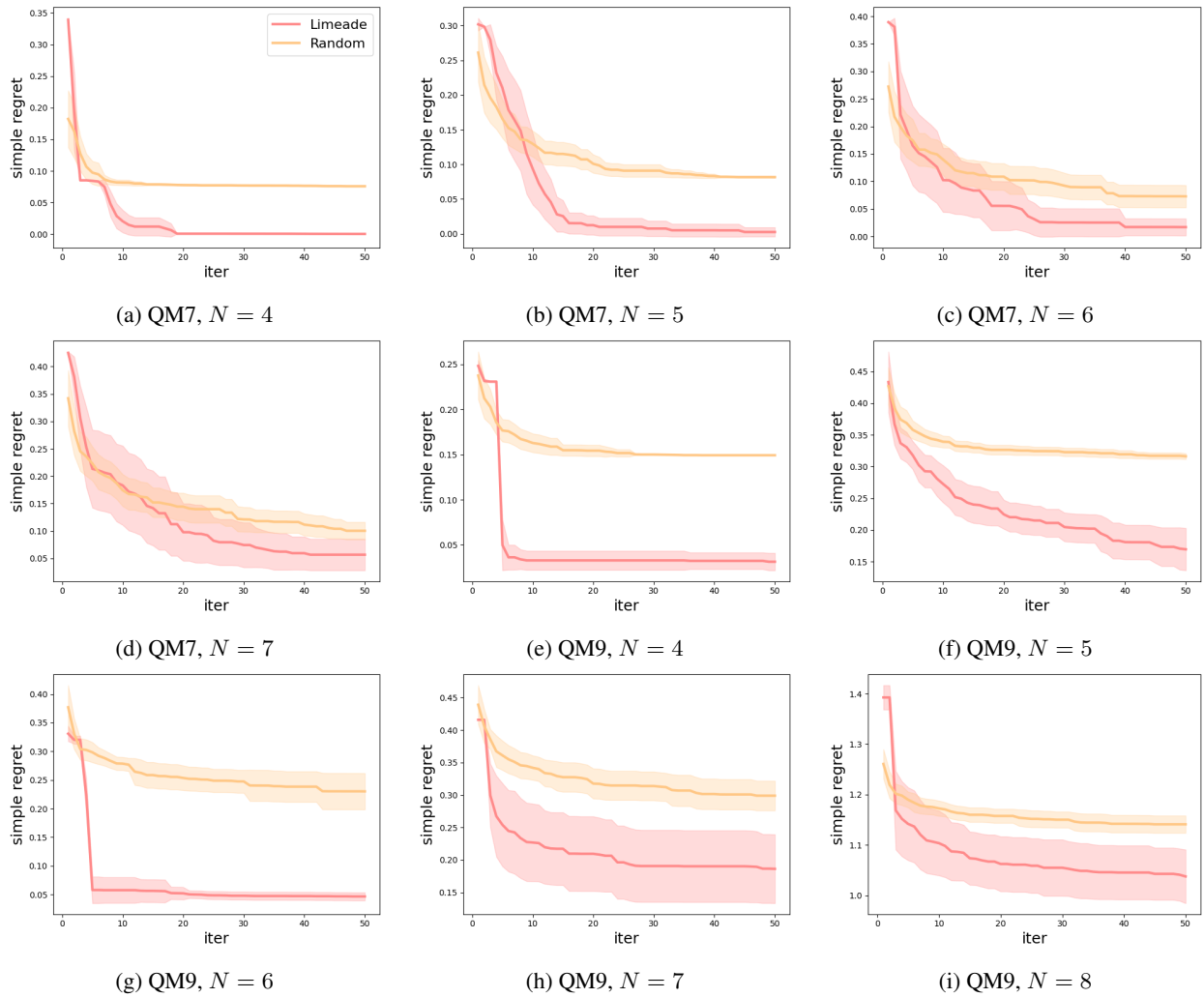
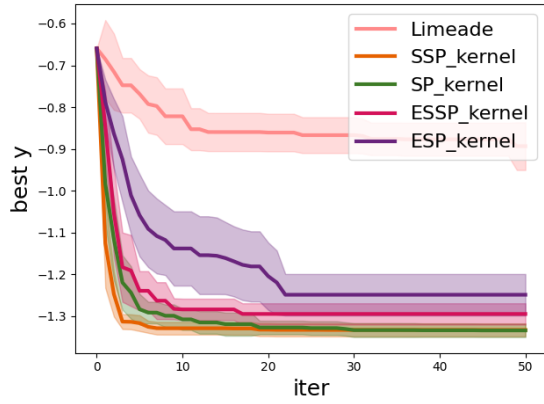
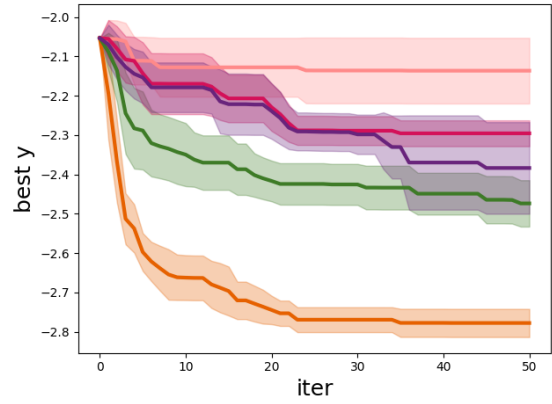


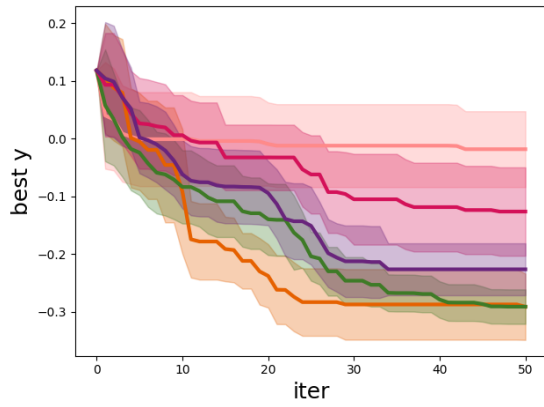
Figure 4: Performance of random sampling and Limeade over QM7 and QM9 datasets with different graph size  $N$ . Simple regret is plotted at each iteration. Mean with 0.5 standard deviation over 10 replications is reported.



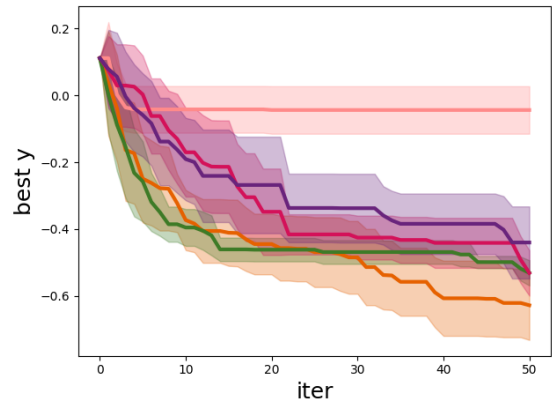
(a) QM7,  $N = 15$



(b) QM7,  $N = 25$



(c) QM9,  $N = 15$



(d) QM9,  $N = 25$

Figure 5: Bayesian optimization results on QM7 and QM9 with  $N \in \{15, 25\}$ . Best objective value is plotted at each iteration. Mean with 0.5 standard deviation over 10 replications is reported.